

# Solar wind – magnetosphere coupling: A review of recent results

T. I. Pulkkinen <sup>a\*</sup>, M. Palmroth<sup>b</sup>, E. I. Tanskanen<sup>b</sup> N. Yu. Ganushkina<sup>b</sup> M. A. Shukhtina<sup>c</sup>, N. P. Dmitrieva<sup>c</sup>

<sup>a</sup>Los Alamos National Laboratory, Los Alamos, NM

<sup>b</sup>Finnish Meteorological Institute, Helsinki, Finland

<sup>c</sup>V. A. Fok Institute of Physics, St.-Petersburg State University, St.-Petersburg, Russia

This paper reviews some aspects of solar wind – magnetosphere – ionosphere interaction. It is shown that in addition to the interplanetary electric field, the solar wind dynamic pressure also has a significant role in determining the state, dynamics, and energetics of the system. It is demonstrated how the state of the magnetosphere and the prior driving affect the amount of energy input to the system, which highlights the capability of the magnetosphere to control the energy flow. The active role of the magnetosphere in determining the dynamics is illustrated by statistical results of the flux balance in the magnetotail and the various dynamic cycles the system can enter. The inner magnetosphere processes during storms are shown to be a result of a complex interplay of processes at the magnetopause and in the magnetotail in response to the solar wind driving. The conclusions are drawn from statistical observational results, empirical models, and global MHD simulations.

## Keywords

substorms, storms, energy budget, magnetotail

## 1. Introduction

Recent results have significantly enhanced our understanding of the dynamic processes within the coupled solar wind – magnetosphere – ionosphere system. However, new questions have emerged and several issues that require global knowledge of the system state remain to be resolved. While the (sequences of the) dynamic processes are easier to address from (multi)point measurements, the energetics of the system is still difficult to address even with the modern fleet of satellites. On the other hand, global magnetohydrodynamic (MHD) simulations (e.g., Janhunen, 1996) are excellent tools to examine the large-scale coupling. Here we focus on comparisons of observational and simulation results and their implications.

Statistical analyses and case studies have highlighted the importance of the solar wind dy-

namic pressure on the magnetospheric configuration, dynamics, and energetics (Lopez et al., 2004; Shukhtina et al., 2004; Palmroth et al., 2004a,b; Siscoe et al., 2005). We address recent results on the interplay of the solar wind and the interplanetary magnetic field (IMF) in driving magnetospheric activity as well as determining its state.

While substorms are global reconfiguration processes, they also represent one of the basic ways by which the magnetosphere processes energy fed in by dayside reconnection during periods of southward interplanetary magnetic field (IMF, Baker et al., 1996). Due to lack of global observations of the system state, many observational analyses have relied on the use of proxies for the energy input and dissipation in the system (Pulkkinen et al., 2006). We address the use of proxies in substorm energetics studies by using global simulations that allow computing both proxies and the true quantities.

As the importance of space weather has grown, the inner magnetosphere processes have been examined using multiple techniques and models. These results have revealed a more complex association of the ring current enhancement, the solar wind parameters, and the tail processes than

---

\*Permanently at: Finnish Meteorological Institute, Helsinki, Finland.

suggested by the highly successful Burton et al. (1975) formulation. We address processes at the magnetopause and in the magnetotail that affect the ring current evolution and discuss their effects on storm dynamics.

## 2. Competing effects of solar wind pressure and interplanetary electric field

The magnetospheric dynamic processes are powered by the IMF embedded in the impinging solar wind flow. As the solar wind flow at Earth orbit is both supersonic and super-Alfvénic, kinetic energy dominates both the energy density ( $\frac{1}{2}\rho V^2 \sim 1.0 \cdot 10^{-9} \text{ J/m}^3$ ,  $B^2/2\mu_0 \sim 1.0 \cdot 10^{-11} \text{ J/m}^3$ ) and energy flux ( $\frac{1}{2}\rho V^3 \sim 5.0 \cdot 10^{-4} \text{ W/m}^2$ ,  $S = E \times B/\mu_0 \sim 1.0 \cdot 10^{-5} \text{ W/m}^2$ ).

The size of the magnetosphere can be determined roughly by setting the subsolar point to where the magnetic pressure of the dipole equals that of the solar wind flow pressure, which gives a dependence  $R_0 \sim P^{-1/6}$ . For typical values, the subsolar point is at about  $10 R_E$ , and the roughly cylindrically symmetric magnetosphere assumes a tail radius of about  $30 R_E$ . Two independent empirical models for the magnetopause position using direct in-situ measurements (Shue et al., 1997) and the total pressure inside the magnetosphere (Shukhtina et al., 2004) are shown in the top panels of Figure 1 for a range of IMF values and for two different values of the pressure. Both yield very consistent results of (a) strong pressure control of the size of the magnetosphere and (b) relatively minor role of the IMF in determining the magnetopause position both at dayside and nightside.

The energy input to the magnetosphere has been parametrized using the solar wind motional electric field  $E_Y = VB_Z$  or the  $\epsilon$  parameter ( $\epsilon = (4\pi/\mu_0)VB^2l_0^2 \sin^4(\theta/2)$ , where  $\theta = \tan^{-1}(B_Y/B_Z)$  is the IMF clock angle), highlighting the importance of dayside reconnection in the energy transfer. The bottom panel of Figure 1 shows a statistical result of the relationship between the merging electric field ( $E_m = VB_t \sin^3(\theta/2)$ , where  $B_t = \sqrt{B_Y^2 + B_Z^2}$ ) and the total tail magnetic flux ( $F_T = \pi R_T^2 B_L/2$ , where  $R_T$  is the tail radius,  $B_L$  the lobe field intensity,

and  $F_T$  contains both open and closed flux). The linear relationship between the tail magnetic flux and the driving solar wind electric field shows that, if the scatter caused by substorms is removed by selecting the flux maxima before the onsets, the dayside reconnection rate quite directly controls the magnetotail flux content in time scales averaged over 1 hour (Shukhtina et al., 2005).

The energy is dissipated via a variety of dynamic processes in the plasma sheet, in the ring current, and in the ionosphere. Because statistical studies have shown that the ionosphere is the dominant energy sink, the ionospheric Joule heating can be used as a proxy for the energy dissipation associated with a substorm (giving a proxy for the "substorm size"). While there is no instantaneous correlation between the driving  $\epsilon$  and the ionospheric dissipation, the time integrals of energy input ( $\int dt\epsilon$ ) and dissipation by ionospheric Joule heating ( $\int dtJH$ ) show a relatively good correlation when the time integration is extended from the time of the substorm onset to the end of the recovery phase (Figure 2a, Tanskanen et al., 2002). Tanskanen et al. further demonstrate that the energy input integrated over the duration of the growth phase plays no role in determining the amount of ionospheric energy dissipation during the expansion and recovery phases. These statistics show that the energy dissipated during the substorm (substorm size) is quite directly controlled by the energy input during the expansion phase, in time scales integrated over the substorm duration.

While it is generally assumed that the solar wind dynamic pressure plays only a minor role in ionospheric Joule heating, a superposed epoch analysis by Palmroth et al. (2004b) show that pressure pulses in the solar wind do cause a signal in the AE index if the IMF has a southward component. Furthermore, global MHD simulations show that the ionospheric dissipation is strongly dependent on the solar wind dynamic pressure, with weaker dependence for northward than for southward IMF (Lopez et al., 2004; Palmroth et al., 2004b). Figure 2b shows a scatter plot of the Joule heating dependence on the instantaneous value of the solar wind pressure, created using

values from many different simulation runs. In the simulation, the region-1 currents connecting to the magnetopause are linearly dependent on the solar wind pressure. As the currents close through the ionosphere, the ionospheric dissipation ( $E \cdot J$ ) is roughly proportional to the square of the current density. Thus, the Chapman-Ferraro current intensity (controlled by the pressure) coupling with the region-1 currents leads to dependence of the ionospheric Joule heating on the dynamic pressure (see also Siscoe et al., 2005). The simulation results suggest a dependence of the ionospheric Joule heating on the solar wind pressure.

### 3. Processes at the magnetopause

While the MHD simulations do not include the detailed reconnection physics at the magnetopause, the numerical effects give rise to reconnection that allows for energy and mass transfer into the magnetosphere. Palmroth et al. (2004a,b) discuss methods to determine the energy input through the GUMICS-4 global MHD simulation magnetopause and its correlations with the energy dissipation in the ionosphere. Figures 3a and b show the energy input through the magnetopause and ionospheric dissipation in a simulation run of a substorm event (Pulkkinen et al., 2006). The thin lines with scale on the right show the observed  $\epsilon$  (proxy for the energy input) and AE index (proxy for the ionospheric dissipation). The lower panels show the relations of the four quantities in a hodogram format revealing their temporal correlations. Note that the  $\epsilon$  can be computed also from the simulation, which allows us to examine the simulation results both using the proxy and the true energy input.

The hodograms show that there is a time-delayed response of the  $\epsilon$  and ionospheric Joule heating as evaluated both from the simulation (Figure 3c) and from observations (Figure 3d). Figure 3e shows that the hysteresis is present already at the magnetopause, as there is a time-delayed response of the energy input through the magnetopause to changes in  $\epsilon$ . Finally, Figure 3f shows that there is an almost linear relationship between the energy input through the mag-

netopause and dissipation in the ionosphere with almost no time delay.

These results indicate that the solar wind and IMF parameters do not alone control the energy transfer through the boundary. On the other hand, energy conversion in the simulation seems to be directly driven by the rate of energy transfer through the boundary. Using  $\epsilon$  and AE as proxies for energy input and dissipation one gets a loading – unloading cycle with increased energy input followed by a later dissipation (both in observations and in the simulation). On the other hand, using the true quantities in the simulation one gets a very nearly directly driven system where the dissipation is controlled by instantaneous energy input. This may indicate that the magnetospheric energetics is more directly driven than the statistical observations using proxies would suggest (Pulkkinen et al., 2006).

### 4. Flux balance in the magnetotail

In a simplistic view, (substorm) activity is required to maintain flux balance in the magnetosphere. The prototypical substorm is often characterized as showing signatures of lobe flux loading together with cross-tail current sheet thinning and intensification (Baker et al., 1996). While the lobe flux loading changes the energy content of the magnetotail, it produces no qualitative change of the magnetotail state. On the other hand, changes in the driving often induce formation of a thin and intense current sheet embedded within the much thicker plasma sheet. The magnetotail can also enter a steady convection (SMC) interval, where the flux transport is in balance for extended periods even when solar wind driving would be sufficient for a substorm to develop (Sergeev et al., 1996). In these cases, the magnetotail flux content does not increase substantially, nor does the current sheet become as thinned as it does during substorm growth phases.

A superposed epoch analysis (Figure 4) illustrates three different responses of the magnetotail, which all have qualitatively similar driver properties: SMC events showing neither loading nor unloading, substorms showing loading and unloading, and substorms not showing loading

(flux balance during the growth phase) but showing unloading after substorm onset. Only a third of substorms show clear lobe field increase and thus significant energy storage (thick lines in Figure 4). On the other hand, the qualitative state change with an embedded thin current sheet is a necessary condition for a substorm to occur. This is clearly shown with strong decrease in  $B_Z$  in both groups of substorm onsets and lack thereof in the case of SMC events (Dmitrieva et al., 2004). As there are no marked differences in the drivers in neither substorm data set nor the SMC event set, these results illustrate the role of the internal magnetospheric processes in controlling the evolution of the dynamics.

## 5. Coupling to the inner magnetosphere

Early studies demonstrated that the ring current intensity (using the Dst index as a proxy) can be derived from the driving interplanetary electric field using  $d\text{Dst}^*/dt = Q(t) - \text{Dst}^*/\tau$ , where  $\text{Dst}^*$  has been corrected for solar wind dynamic pressure effects by  $\text{Dst}^* = \text{Dst} - b\sqrt{P} + c$  and the source function  $Q(t)$  is a linear function of the driver  $VB_s$  (Burton et al., 1975; O'Brien and McPherron, 2000). The interpretation of this result is that the interplanetary electric field penetrates to the plasma sheet, where enhanced convection drives particles to the inner magnetosphere and increase the ring current.

Recently, Siscoe et al. (2005) argued that the pressure correction in the Burton et al. formulation is not a constant, but depends on the driver intensity ( $b = b(E_y)$ ). They suggest that  $b$  is largest for small  $E_y$  and goes to virtually zero as  $E_y$  increases. They argue that the dayside current systems change during storms: The compression produced by the dynamic pressure is no longer increasing the Chapman-Ferraro currents at the magnetopause, but rather enhance region-1 currents coupling to the ionosphere. This way the magnetosphere can limit the compression that the IMF and solar wind can produce. As the pressure correction makes Dst more negative, this would imply that the ring current intensity derived from  $\text{Dst}^*$  is an overestimate.

A statistical study of ring current acceleration

during storms showed that the initial ring current intensification consists of ions in the energy range of tens of kilovolts. During the storm recovery, the ring current characteristic energy increases such that a major contribution to the energy density comes from higher energy particles having energies exceeding 100 keV (Ganushkina et al., 2004). Figure 5 shows results from drift computations attempting to reproduce the observed characteristics of the ring current energy distribution. The black curves show the time evolution of the ring current energy during a double storm, the colored curves show contributions from low (blue), medium (green) and high (red) energy particles. Figure 5a shows a computation using a large-scale convection electric field to drive the particle motion. Figure 5b shows the same calculation, but now in addition to the convection electric field, traveling electric field pulses representing substorms have been added to the model. It is evident that after the second storm peak, Figure 5b shows much larger increase of the energy in the highest-energy particles (red curves). Ganushkina et al. (2004) conclude that the localized, pulsed electric fields are necessary to create the high-energy population in the ring current. This result also provides an explanation why the SMC periods have lower than expected effect on the Dst index and ring current, as there by definition are no substorms during the SMC periods.

## 6. Discussion and conclusions

The magnetospheric state is a result of complex interactions of the driving solar wind and IMF with the magnetosphere – ionosphere system. Pressure balance arguments can be used to explain the dominant role of the solar wind dynamic pressure in determining the magnetospheric size (Figure 1; Shukhtina et al., 2004). However, during storms the relative intensities of the Chapman-Ferraro and region-1 currents change (Siscoe et al., 2005), which leads to smaller than expected compression of the magnetosphere. Thus, during storms the standoff distance is determined by the combined effects of the pressure and the southward IMF. On the other hand, the solar wind electric field is the main

driver of both the tail magnetic flux content (Figure 1; Shukhtina et al., 2005; Milan et al., 2004) and ring current intensity (O’Brien and McPherron, 2000).

The substorm, representing a basic dynamic process in the magnetosphere, comprises preconditioning to a metastable state followed by an explosive reconfiguration and slow recovery. Statistical results indicate that the only necessary condition for a substorm to occur is the formation of a thin and intense current sheet in the plasma sheet (Dmitrieva et al., 2004). Because not all substorms are associated with tail flux loading and because the thinning is much stronger than that caused by compression by added tail flux, the thin current sheet formation is likely driven by changes in the tail boundary conditions (Schindler and Birn, 1993). It may be that instabilities related to non-adiabatic ion motion within the thin current sheet are associated with the substorm onset process (e.g., Pulkkinen et al., 1992).

The state of the magnetosphere controls the effects of the flux loading in multiple ways. At the magnetopause, the energy transfer rate is dependent on the state of the system (Figure 3; Pulkkinen et al., 2006). The balance between dayside and nightside reconnection is also dependent on the history and state of the tail, in a way yet to be determined. Steady convection events can maintain flux balance for extended periods without significant loading even if the IMF remains steadily southward (Sergeev et al., 1996). Substorms may occur with or without significant flux imbalance; only about a third of substorms show prior flux loading (Figure 4; Dmitrieva et al., 2004). Furthermore, there does not seem to be a limit value of tail flux for a substorm to occur; increased driving leads to increased tail flux content (Figure 1; Shukhtina et al., 2005).

Even if storms seemingly are quite directly driven (O’Brien and McPherron, 2000), the ring current accumulation is coupled to the tail processes through substorm activity: small-scale electric fields are required to energize the particles to the observed high energies (Figure 5; Ganushkina et al., 2004). Slowly varying convection alone is not capable of producing the high-energy ring current, which is further demon-

strated by the lower than expected Dst response during the SMC events.

The use of proxies such as  $\epsilon$  and  $AE$  has led to the notion that the substorm energy cycle is to store energy during the growth phase and release that energy during the expansion and recovery phases. However, statistical studies of the substorm size or ionospheric dissipation show that this is not the case; the substorm size is determined by the amount of energy input after, not before, the onset time (Figure 2; Tanskanen et al., 2002). Furthermore, observations have shown that the solar wind dynamic pressure is also a factor in determining the amount of ionospheric dissipation (Palmroth et al., 2004b).

Global MHD simulations add interesting aspects on these issues: First, the simulation results show that the ionospheric dissipation is directly proportional to the solar wind pressure, which can be explained by the coupling via the region-1 currents (Figure 2; Palmroth et al., 2004b). This result may be overemphasized in the global MHD simulations where the region-2 current systems are weak, but has been shown to be significant in strongly driven storms (Lopez et al., 2004). Secondly, it seems that the level of prior energy input controls energy transfer across the magnetopause (Figure 3; Pulkkinen et al., 2006); Palmroth et al. (2006) discuss the origins of the effect and demonstrate that the same is true for a variety of simulation runs. The results indicate that the amount of dissipation is quite directly controlled by the rate of energy input through the boundary. As comparison of  $\epsilon$  and ionospheric dissipation give similar results in simulations and observations, this may indicate that the substorm energetics is quite directly driven by the true energy input through the boundary.

The dependence of the pressure correction on the driving  $E_Y$  brings an important aspect to storm energetics: If the pressure correction to the Dst index is small during storms, the ring current is not as strong as assumed using Dst as a proxy, because the pressure correction is in the direction as to increase the absolute value of the Dst index. Thus, the role of the ring current as an energy sink needs to be re-evaluated especially during storms with high dynamic pressure when

the pressure correction can be several tens of nT.

The above highlights in multiple ways the coupled and complex nature of magnetospheric processes. Especially, it seems that the use of proxies in lieu of actual global measurements may have yielded misleading results of substorm energetics, which seems to be more directly driven than has been thought before. As the dynamic substorm process is very much one of pre-conditioning – explosive reconfiguration, it is important to note that the energetics and dynamics need not show similar behavior. The interlinked effects of pressure and electric field on the dynamics as well as energetics, and the high degree of coupling between processes in the solar wind, at the magnetospheric boundaries, in the tail, inner magnetosphere and ionosphere poses significant challenges in modeling this vast system; either global models or careful consideration of boundary conditions in local models are required for improved understanding of our space environment.

## REFERENCES

1. Baker, D. N., T. I. Pulkkinen, V. Angelopoulos, W. Baumjohann, and R. L. McPherron, The neutral line model of substorms: Past results and present view, *J. Geophys. Res.*, *101*, 12,975, 1996.
2. Boyle, C. B., P. H. Reiff, and M. R. Hairston, Empirical polar cap potentials, *J. Geophys. Res.*, *102*, 111, 1997.
3. Burton, R. K., R. L. McPherron, and C. T. Russell, An empirical relationship between interplanetary conditions and Dst, *J. Geophys. Res.*, *80*, 4204, 1975.
4. Dmitreva, N. P., V. A. Sergeev, and M. A. Shukhtina, Average characteristics of the midtail plasma sheet in different dynamic regimes of the magnetosphere, *Ann. Geophys.*, *22*, 2107, SRef-ID: 1432-0576/ag/2004-22-2107, 2004.
5. Gamushkina, N. Yu., T. I. Pulkkinen, M. V. Kubyshkina, H. J. Singer, and C. T. Russell, Long-term evolution of magnetospheric current systems during storm periods, *Ann. Geophys.*, *22*, 1317, 2004.
6. Janhunen, P., GUMICS-3: A global ionosphere-magnetosphere coupling simulation with high ionospheric resolution, in *Proceedings of Environmental Modelling for Space-based Applications*, ESA-SP 392, p. 205, 1996.
7. Lopez, R. E., S. Hernandez, J. G. Lyon, M. Wiltberger, Solar wind density control of energy transfer to the magnetosphere, *Geophysical Research Letters*, *31*, L08804, DOI: 10.1029/2003GL018780, 2004.
8. Milan, S. E., Dayside and nightside contributions to the cross polar cap potential: placing an upper limit on a viscous-like interaction, *Ann. Geophys.*, *22*, 3771, 2004. SRef-ID: 1432-0576/ag/2004-22-3771.
9. O'Brien, P., and R. L. McPherron, An empirical phase space analysis of ring current dynamics: Solar wind control of injection and decay, *J. Geophys. Res.*, *105*, 7707, doi:10.1029/1998JA000437, 2000.
10. Palmroth, M., P. Janhunen, T. I. Pulkkinen, and H. E. J. Koskinen, Ionospheric energy input as a function of solar wind parameters: global MHD simulation results, *Ann. Geophys.*, *22*, 549, 2004a.
11. Palmroth, M., T. I. Pulkkinen, P. Janhunen, D. J. McComas, C. W. Smith, and H. E. J. Koskinen, Role of solar wind dynamic pressure in driving ionospheric Joule heating, *J. Geophys. Res.*, *109*, A11302, doi:10.1029/2004JA010529, 2004b.
12. Palmroth, M., P. Janhunen, and T. I. Pulkkinen, Hysteresis in the solar wind power input into the magnetosphere, *Geophys. Res. Lett.*, *33*, L03107, doi:10.1029/2005GL025188, 2006.
13. Pulkkinen, T. I., D. N. Baker, R. J. Pellinen, J. Büchner, H. E. J. Koskinen, R. E. Lopez, R. L. Dyson, and L. A. Frank, Particle scattering and current sheet stability in the geomagnetic tail during the substorm growth phase, *J. Geophys. Res.*, *97*, 19,283, 1992.
14. Pulkkinen, T. I., M. Palmroth, E. I. Tanakanen, P. Janhunen, H. E. J. Koskinen, and T. V. Laitinen, New interpretation of magnetospheric energy circulation, *Geophys. Res. Lett.*, *33*, L07101, doi:10.1029/2005GL025457, 2006.

15. Schindler, K., and J. Birn, On the cause of thin current sheets in the near-Earth magnetotail and their possible significance for magnetospheric substorms, *J. Geophys. Res.*, *98*, 15477, 1993.
16. Sergeev, V. A., T. I. Pulkkinen, and R. J. Pellinen, Steady magnetospheric convection: A review of recent results, *Space Sci. Rev.*, *75*, 551, 1996.
17. Shue, J.-H., J. K. Chao, H. C. Fu, C. T. Russell, P. Song, K. K. Khurana, and H. J. Singer, A new functional form to study the solar wind control of the magnetopause size and shape, *J. Geophys. Res.*, *102*, 9497, 1997.
18. Shukhtina, M. A., N. P. Dmitrieva, and V. A. Sergeev, Quantitative characteristics of different magnetospheric states, *Ann. Geophys.*, *22* 1019, SRef-ID: 1432-0576/ag/2004-22-1019, 2004.
19. Shukhtina, M. A., N. P. Dmitreva, N. G. Popova, V. A. Sergeev, A. G. Yahnin, and I. V. Despirak, Observational evidence of the loading-unloading substorm scheme, *Geophys. Res. Lett.*, *32*, L17107, doi:10.1029/2005GL023779, 2005.
20. Siscoe, G. L., R. L. McPherron, and V. K. Jordanova, Diminished contribution of ram pressure to Dst during magnetic storms, *J. Geophys. Res.*, *110*, A12227, doi:10.1029/2005JA011120, 2005.
21. Tanskanen, E. I., T. I. Pulkkinen, H. E. J. Koskinen, Substorm energy budget near solar minimum and maximum: 1997 and 1999 compared, *J. Geophys. Res.*, *107*, A6, doi:10.1029/2001JA900153, 2002.

## 7. Figure captions

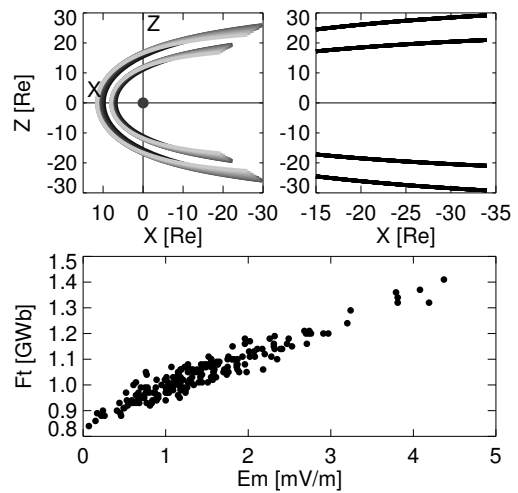


Figure 1. Solar wind and IMF control of the magnetosphere: (Top) Magnetopause location from the empirical (left) Shue et al. (1997) and (right) Shukhtina et al. (2004) models for  $P_{SW}=1$  and 11 nPa and  $B_Z = -10...10$  nT. (Bottom) Observational statistics of tail magnetic flux  $F_T$  at substorm onset as a function of merging electric field  $E_m$  (averaged for 1 hour prior to substorm onset, for definitions see text, after Shukhtina et al., 2005).

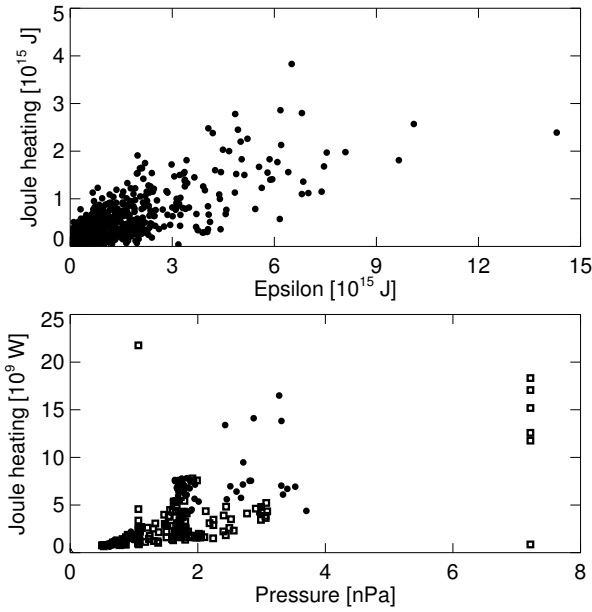


Figure 2. Ionospheric energy dissipation: (a) Observed time-integrated ionospheric energy dissipation (in Joule, using proxy  $\int dt 3 \cdot 10^8 AL$ ) as a function of time-integrated driving  $\epsilon$  (in Joule) (after Tanskanen et al., 2002). (b) Dependence of the instantaneous ionospheric Joule heating power (in Watt) on the solar wind dynamic pressure in the GUMICS-4 global MHD simulation, for  $B_Z \leq 0$  (filled circles) and for  $B_Z > 0$  (open squares) (after Palmroth et al., 2004b).

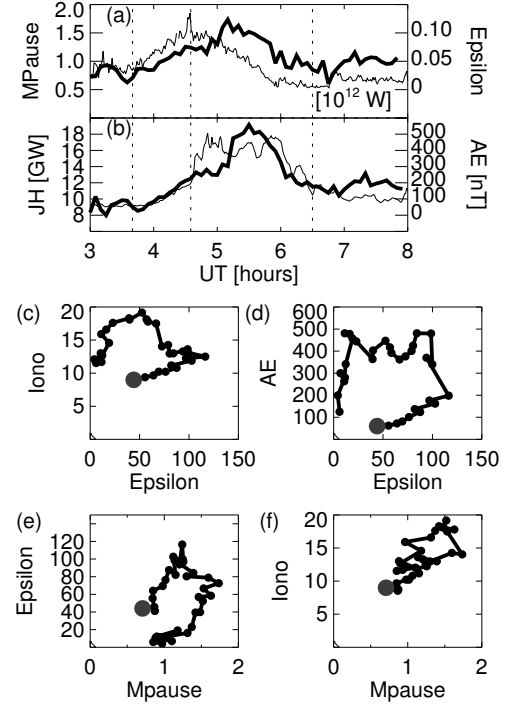


Figure 3. Energy transfer during a substorm on Aug 15, 2001 in the GUMICS-4 global MHD simulation: (a) Energy transfer rate (power) through the magnetopause in  $10^{12}$  W from the simulation (thick line) and  $\epsilon$  in  $10^{12}$  W (thin line, scale on the right). (b) Ionospheric Joule heating in GW from the simulation (thick line) and AE in nT (thin line, scale on the right). (c) Epsilon [GW] vs. ionospheric Joule heating [GW] from the simulation. (d) Epsilon [GW] vs. AE [nT] from observations. (e) Energy transfer rate [ $10^{12}$  W] vs. Epsilon [GW] from the simulation. (f) Energy transfer rate [ $10^{12}$  W] vs. ionospheric Joule heating [GW] from the simulation. The large dot shows the time at the beginning of the event (after Pulkkinen et al., 2006).

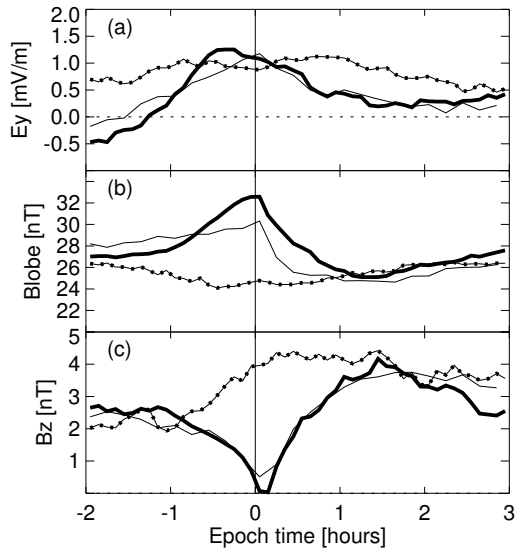


Figure 4. Tail flux balance: Superposed epoch analysis using Geotail data. (a) Driving solar wind motional electric field  $E_Y$ , (b) tail lobe magnetic field, and (c)  $B_Z$  in plasma sheet for substorms with flux loading (thick solid line), substorms with no flux loading (thin solid line) and SMC events (dotted line) (note that the SMC event begins at time  $T_0$ ; after Dmitrieva et al., 2004).

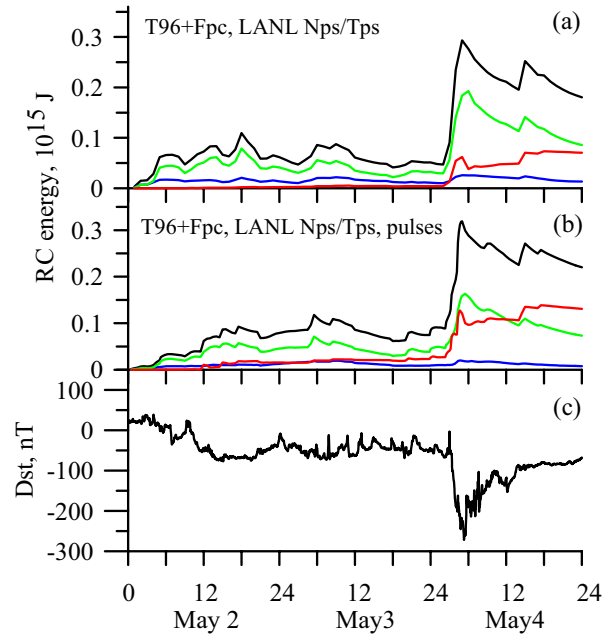


Figure 5. Inner magnetosphere coupling: May 2–4, 1998. Energy of the ring current for low-energy particles (1–20 keV, blue), medium energies (20–80 keV, green), high energies (80–200 keV, red), and total energy (1–200 keV, black). (a) Time stationary magnetic field, solar wind driven convection electric field. (b) As in top panel, but localized pulses representing substorms added. (c) Dst index for the event. The drift calculations were done using the T96 magnetic field, Boyle et al. (1997) ionospheric potential mapped to the magnetotail, and LANL MPA measurements to give boundary conditions (after Ganushkina et al., 2004).